

# Spin-splitting in the quantum Hall effect of disordered GaAs layers with strong overlap of the spin subbands

S. S. Murzin<sup>1,2</sup>, M. Weiss<sup>2</sup>, D. A. Knyazev<sup>1</sup>, A. G. M. Jansen<sup>2,3</sup>, and K. Eberl<sup>4</sup>

<sup>1</sup>*Institute of Solid State Physics RAS, 142432, Chernogolovka, Moscow District., Russia*

<sup>2</sup>*Grenoble High Magnetic Field Laboratory, Max-Planck-Institut für Festkörperforschung and Centre National de la Recherche Scientifique, BP 166, F-38042, Grenoble Cedex 9, France*

<sup>3</sup>*Service de Physique Statistique, Magnétisme, et Supraconductivité, Département de Recherche Fondamentale sur la Matière Condensée, CEA-Grenoble, 38054 Grenoble Cedex 9, France*

<sup>4</sup>*Max-Planck-Institut für Festkörperforschung, Postfach 800 665 D-70569, Stuttgart, Germany*

With minima in the diagonal conductance  $G_{xx}$  and in the absolute value of the derivative  $|dG_{xy}/dB|$  at the Hall conductance value  $G_{xy} = e^2/h$ , spin-splitting is observed in the quantum Hall effect of heavily Si-doped GaAs layers with low electron mobility  $\mu \approx 2000 \text{ cm}^2/\text{Vs}$  in spite of the fact that the spin-splitting is much smaller than the level broadening. Experimental results can be explained in the frame of the scaling theory of the quantum Hall effect, applied independently to each of the two spin subbands.

PACS numbers: PACS numbers: 71.30.1+h, 73.43.2-f

In an electron system with a small  $g$ -factor strong disorder broadens and suppresses the spin-split structure in the electron spectrum in an applied magnetic field. Therefore, spin-splitting with Zeeman energy separation  $E_s = g\mu_B B$  ( $\mu_B$  is the Bohr magneton and  $B$  the magnetic field) does not show up in the kinetic and thermodynamic properties of strongly disordered 3D bulk electron systems. However, for a 2D system, the scaling theory for diffusive interference effects leads to a quite unexpected conclusion: the spin-splitting can arise in the magneto-quantum transport data even in the case of very small  $E_s$  with respect to energy-level broadening  $\Gamma$  if the temperature is sufficiently low. For this situation with  $E_s \ll \Gamma$ , the spin-split quantum Hall effect (QHE) with odd integer Hall-conductance plateaux at  $G_{xy} = (2i + 1)e^2/h$  and corresponding minima in the diagonal conductance (per square)  $G_{xx}$  should develop at low temperatures due to the existence of extended states near the center of two spin-split Landau levels with localized states in between [1, 2]. However, the spin-splitting was not observed in disordered 2D GaAs systems with mobilities below  $10000 \text{ cm}^2/\text{Vs}$  [3] when  $E_s \ll \Gamma$ . Higher mobility samples generally do show the spin-splitting [4] due to the enhanced Zeeman splitting in such pure two dimensional samples because of electron-electron interaction effects [5]. Strong disorder should suppress this enhancement of spin-splitting [6].

In the present work we observed for the first time the manifestation of the spin-splitting in the magneto-conductance of a strongly disordered system, a heavily Si-doped GaAs layer with a low electron mobility  $\mu \approx 2000 \text{ cm}^2/\text{Vs}$ . For the case of these layers, the spin-splitting  $E_s$ , with  $E_s/k_B$  about 4 K at a magnetic fields of  $B = 12 \div 13 \text{ T}$ , is much smaller than the level broadening  $\Gamma$  ( $\gtrsim 100 \text{ K}$ ) resulting in a strong overlap of the two spin subbands. We analyzed the scaling properties of the transport data of our electron system with weak spin-splitting, assuming that the conductances of the different spin subbands are renormalized independently for

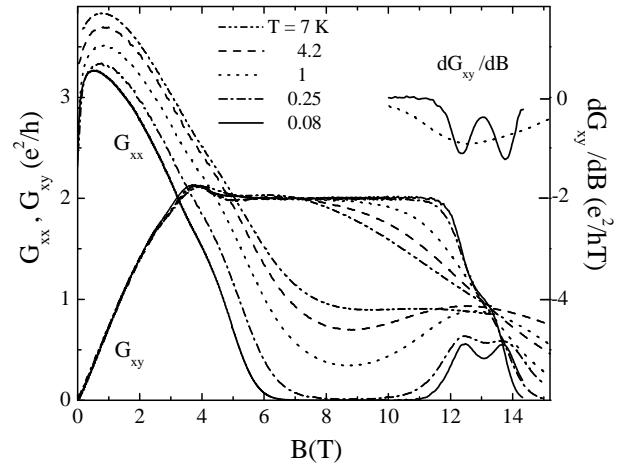


FIG. 1: Magnetic field dependence of the diagonal ( $G_{xx}$ ) and Hall ( $G_{xy}$ ) conductance, and of derivative  $dG_{xy}/dB$  for sample 40 in a magnetic field perpendicular to the heavily doped GaAs layer (thickness 40 nm) at different temperatures, showing spin-splitting for  $G_{xy} = 1$  at 13 T.

variations due to diffusive interference effects. Such an approach is justified in the absence of spin-flip scattering, at least, for non-interacting electrons. Experimental data are in accordance with such an analysis.

The investigated heavily Si-doped n-type GaAs layers sandwiched between undoped GaAs were prepared by molecular-beam epitaxy. The number given for a sample corresponds to the thickness  $d$  of the conducting doped layers with  $d = 34, 40, \text{ and } 50 \text{ nm}$ . The Si-donor concentration is  $1.5 \times 10^{17} \text{ cm}^{-3}$ . Hall bar geometries of width 0.2 mm and length 2.8 mm were etched out of the wafers. A phase sensitive ac-technique was used for the magneto-transport measurements down to 40 mK with the applied magnetic field up to 20 T perpendicular to the layers.

The electron densities per square as derived from the slope of the Hall resistance  $R_{xy}$  in weak magnetic fields

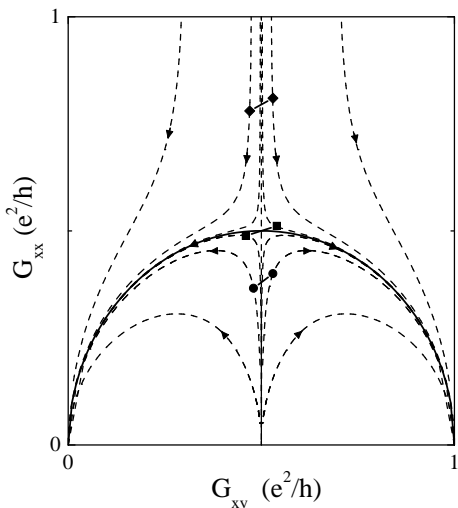


FIG. 2: Theoretical flow lines [7] showing the coupled evolution of the diagonal ( $G_{xx}$ ) and Hall conductance ( $G_{xy}$ ) for a totally spin polarized electron system. The arrows indicate the direction of flow for decreasing temperature. Pairs of diamonds, squares and circles indicate possible starting positions ( $G_{xy}^-, G_{xx}^-$ ) and ( $G_{xy}^+, G_{xx}^+$ ) for the scaling in the cases (i), (ii), and (iii), respectively, as described in the text.

(0.5 – 3 T) at  $T = 4.2$  K are  $N_s = 3.9, 4.6$  and  $5.0 \times 10^{11} \text{ cm}^{-2}$  for samples 34, 40 and 50, respectively. The bare high temperature mobilities  $\mu_0$  are about 2000, 2200 and  $2400 \text{ cm}^2/\text{Vs}$ . Because of the rather large quantum corrections to the conductance, even in zero magnetic field at 4.2 K, we used for determining the mobility the approximate relation  $\mu_0 = R_{xy}/BR_{xx}$  at the intersection point of the  $R_{xx}(B)$  curves for different temperatures.

The characteristic energy scales of our samples with not more than two size-quantized energy levels are as follows. The Fermi energy at zero magnetic field  $E_F/k_B \approx 200$  K, the splitting of the size quantization  $E_{sq}/k_B = 3(\pi\hbar/d)^2/2mk_B \approx 100 \div 200$  K (for our thinnest sample with  $E_{sq}/k_B \approx 200$  K the second subband is occupied due to disorder),  $\hbar/\tau k_B \approx 100$  K ( $\tau$  is the transport relaxation time at zero magnetic field), the Landau-level energy broadening  $\Gamma/k_B = \hbar\sqrt{2\omega_c}/\pi\tau/k_B \approx 130$  K, and cyclotron energy  $\hbar\omega_c/k_B \approx 250$  K at the magnetic field  $B = 12 \div 13$  T.

The magnetoconductance data for the three samples are rather similar. In Fig.1 the diagonal ( $G_{xx}$ ) and Hall ( $G_{xy}$ ) conductance as calculated from the diagonal per square ( $R_{xx}$ ) and Hall ( $R_{xy}$ ) resistance have been plotted for sample 40. At low temperatures the curves  $G_{xy}(B)$  show a wide QHE plateau from  $\approx 6$  up to  $\approx 11.5$  T with the value of  $G_{xy} = 2$  accompanied by an exponentially small value of  $G_{xx}$  at low temperatures  $T \lesssim 0.3$  K [8]. At the lowest temperature the diagonal ( $G_{xx}$ ) conductance and derivative  $|\partial G_{xy}/\partial B|$  show minima at  $B \approx 13$  T where at high temperature the Hall conductance  $G_{xy} \approx 1$ . The value of the magnetic field where the spin-split QHE is observed is only 1.5 times larger than the QHE

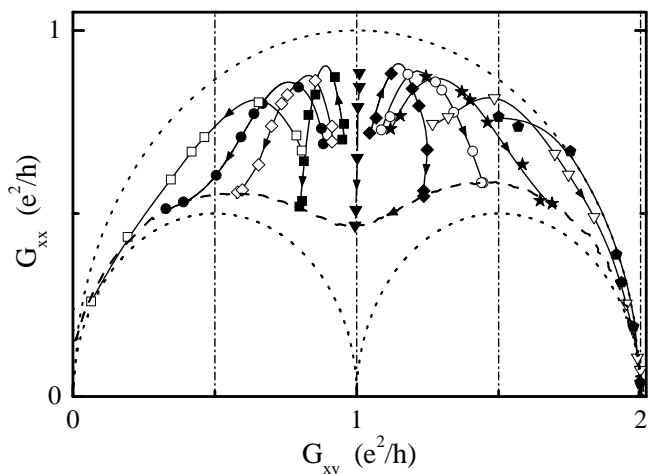


FIG. 3: Flow-diagram of the ( $G_{xx}(T), G_{xy}(T)$ ) data points for sample 34 with decreasing temperature (arrows) from 12 down to 0.1 K. Different symbols connected by solid lines are for different magnetic fields from 9 to 13 T. Dotted lines show the semicircles (Eq.1) and a two times larger one. The dashed line shows the magnetic-field-driven diagonal conductance  $G_{xx}(G_{xy})$  from 8 to 13.8 T at  $T = 0.1$  K. Vertical dash-dotted grid lines are plotted for reference.

field with  $G_{xy} = 2$ , which should be compared with the factor 2 expected from filling-factor related arguments.

The scaling treatment of the QHE [9] results in a graphical presentation of the flow diagram [10] which depicts the coupled evolution of the diagonal ( $G_{xx}$ ) and Hall ( $G_{xy}$ ) conductance components with increasing coherence length. Recent developments [7] of the scaling theory based on symmetry arguments resulted in a calculation of the exact shape of the flow lines  $G_{xx}(G_{xy})$  for a totally spin polarized electron system as plotted in Fig.2 for  $0 \leq G_{xy} \leq 1$ . The different quantum Hall phases ( $i = 0, 1, \dots$ ) in the flow diagram are separated by the vertical lines  $G_{xy} = i + 1/2$ . At sufficiently low temperatures the ( $G_{xx}, G_{xy}$ ) data flow on a separatrix in the form of a semicircle

$$G_{xx}^2 + [G_{xy} - (i + 1/2)]^2 = 1/4. \quad (1)$$

Critical points can be found at  $(G_{xy}^c, G_{xx}^c) = (i + 1/2, 1/2)$ . The same critical positions were found in microscopic descriptions of the QHE for the case of non-interacting electrons [12, 13].

In Fig.3 we have plotted the flow lines showing the temperature evolution of the points ( $G_{xy}(T), G_{xx}(T)$ ) of conductance for sample 34 at different magnetic fields with temperature ranging from  $\approx 10$  down to  $\approx 0.1$  K. For sample 40, the flow diagram is rather similar to one for sample 34. For these samples, at the magnetic fields where the spin-splitting is observed, the flow lines move upwards and then downwards for decreasing temperatures. The lines cross each other for data at different magnetic fields, in contrast to the theoretical prediction for the case of a totally spin polarized electron

system (see Fig.2). For sample 50, the flow lines do not show the upward trend and are not crossing each other. For low temperatures (below 3 K) the flow diagrams are very similar for all three samples: the flow lines approach the semicircles according Eq.1. Linear extrapolation of  $G_{xx}(T)$  and  $G_{xy}(T)$  from 0.5 to 0 K at the two fields where  $G_{xx}(B)$  has a maximum (see Fig.1) results in values  $G_{xx} = 0.5 \pm 0.02$ ,  $G_{xy} = 0.5 \pm 0.05$  and  $1.5 \pm 0.05$ . These critical values are the same as predicted for a totally spin polarized electron system. At the lowest temperatures, the magnetic-field driven dependence  $G_{xx}(G_{xy})$  is mostly not far from the two smaller semicircles (Eq.1) shown in Fig.3 by the dashed lines.

In the absence of spin-flip scattering, the conductances of the different spin subbands are renormalized independently, at least, for the case of non-interacting electrons. Since the temperature dependence of the magnetoconductance is not known for a single spin-polarized band, it is impossible to estimate accurately the flow lines for the total conductance from the flow lines for the single polarized bands because the summation  $G_{ij}(T) = G_{ij}^-(T) + G_{ij}^+(T)$  involves different positions on the spin-polarized flow lines at the same temperature. The index + and - correspond to the majority and minority spin subsystems with larger and smaller Hall conductances, respectively. Nevertheless we can do some conclusions about the scaling properties of the total conductance  $G_{ij}$ .

For weak spin-splitting  $g\mu_B B \ll \hbar/\tau \lesssim E_F$  the bare (non-renormalized) conductances  $G_{ij}^{0\pm}$  for the two spin subbands as measured at high temperatures

$$G_{ij}^{0\pm} = \frac{G_{ij}^0}{2} \pm \frac{g\mu_B B}{4} \frac{\partial G_{ij}^0}{\partial E}, \quad (2)$$

differ weakly from each other because  $g\mu_B B \partial G_{ij}^0 / \partial E \sim G_{ij}^0 g\mu_B B / \Gamma \ll G_{ij}^0$ . Here  $G_{ij}^0 = G_{ij}^{0-} + G_{ij}^{0+}$  and  $E_F$  the Fermi energy. The QHE with total Hall conductance  $G_{xy} = 1$  should arise when one subsystem is in the insulator state ( $(G_{xy}^-, G_{xx}^-) \rightarrow (0,0)$  for  $T \rightarrow 0$ ) (see Fig.2 for the conductances of a single spin-polarized band), and the other in the QHE state ( $(G_{xy}^+, G_{xx}^+) \rightarrow (1,0)$ ). This occurs in a narrow magnetic field range where  $G_{xy}^{+0} > 1/2$  but  $G_{xy}^{-0} < 1/2$ . At the critical value of  $G_{xy}^{-0} = 1/2$  and  $G_{xy}^{+0} > 1/2$ ,  $(G_{xy}^-, G_{xx}^-) \rightarrow (1/2, 1/2)$  and  $(G_{xy}^+, G_{xx}^+) \rightarrow (1,0)$ , therefore, the total conductance  $(G_{xy}, G_{xx}) \rightarrow (3/2, 1/2)$ . Similarly, at the critical value of  $G_{xy}^{+0} = 1/2$ , the total conductance  $(G_{xy}, G_{xx}) \rightarrow (1/2, 1/2)$ . Thus, the critical points are the same as for the case of a totally spin polarized electron system, in accordance with experimental results. This differs from the situation for the distorted flow diagram predicted for the case of small spin-splitting compared to the cyclotron energy ( $g\mu_b B < \hbar\omega_c$  [11]), leading to essentially different positions of the critical points whose exact position depends on the amount of spin-splitting. Note, that these results [11] have been obtained on the basis of a postulated symmetry group in order to include spin-splitting, without giving any microscopic picture for the scaling behavior.

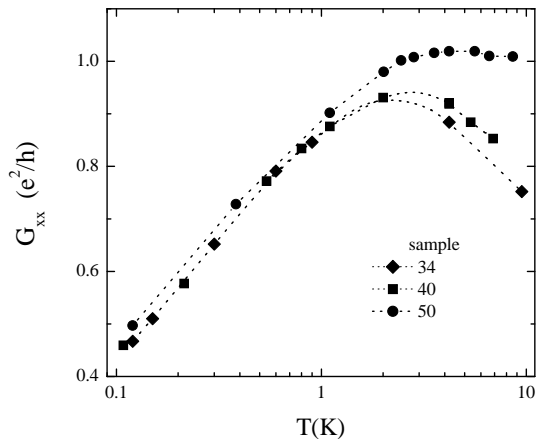


FIG. 4: Temperature dependence of the diagonal ( $G_{xx}$ ) conductance, for sample 34 (diamonds), 40 (squares), and 50 (circles) at a magnetic field  $B = 13.1$  T where the spin-split structure is observed.

At low enough temperatures, when the spin-split QHE is well developed so that in the QHE minimum  $G_{xx} \approx 0$ , one can argue that the flow lines should follow the lines derived for the case of a totally spin polarized electron system. In the minimum of  $G_{xx}$  holds  $(G_{xy}^-, G_{xx}^-) = (0,0)$  and  $(G_{xy}^+, G_{xx}^+) = (1,0)$ , i.e. the minority subsystem does not contribute to conductance and the majority subsystem contributes only the quantum value  $G_{xy} = 1$  to the Hall conductance. At lower magnetic fields, the + subsystem contributes only to the Hall conductance the value 1 as before, and the total conductance  $(G_{xy}, G_{xx}) = (G_{xy}^- + 1, G_{xx}^-)$ . Similarly, at higher magnetic fields  $(G_{xy}, G_{xx}) = (G_{xy}^+, G_{xx}^+)$ . At the lowest temperatures, the total conductance  $(G_{xy}, G_{xx})$  is expected to flow along the same lines as derived for a single spin-polarized electron system. Therefore,  $G_{xx}$  as a function of  $G_{xy}$  flows for a changing magnetic field close to the semicircles given by Eq.1, in accordance with experimental data below 0.1 K.

As mentioned above, for the totally spin polarized electron system, the flow lines should not cross each other [10] in contrast to our experimental data. For the case of two different spin projections, we will show now that the flow lines starting in the region in between the large semicircle and the two smaller semicircles shown in Fig.3 can cross each other. Consider the line ending at the critical point  $(0.5, 0.5)$  as a reference line. Starting slightly at the left from the starting point of this line, and knowing that this line should end at  $(0,0)$ , the crossing is unavoidable. Starting at the right from the starting point of this reference line, and knowing that this line should end at  $(1,0)$ , leads also to a crossing point.

The scaling theory predicts different type of the temperature dependence  $G_{xx}(T)$  in the magnetic-field region where  $G_{xy}^0$  is close to 0.5 for the case of the totally spin-polarized electron system. (i) For  $G_{xx}^0 > 0.5$  flow lines go down, i.e.  $G_{xx}$  decreases with decreasing temperature as

shown in Fig.2 for points starting at the diamonds. (ii) For  $G_{xx}^0 \approx 0.5$  flow lines start nearly horizontally near the maximum of the semicircle (starting at the squares in Fig.2) leading to a very weak temperature dependence of  $G_{xx}(T)$  followed by a decrease at lower temperatures. (iii) For  $G_{xx}^0 < 0.5$  the flow lines go up to a value of  $G_{xx}$  close to 0.5 and then down, i.e.  $G_{xx}$  at first increases with decreasing temperature and then decreases with a maximum value of the diagonal conductance  $\approx 0.5$ . For the case of two spin-subbands with small spin-splitting the above description remains valid for the conductances of the two spin polarizations adding up to the measured total conductance. The Hall conductance should depend weakly on temperature in all these cases, because  $G_{xy}^-$  decreases and  $G_{xy}^+$  increases with decreasing temperature.

In Fig.4 we plot the diagonal conductance  $G_{xx}$  as a function of temperature  $T$  in the spin-split minima of  $G_{xx}$  where  $G_{xy}^0 \approx 1$  for the three samples. The data are in accordance with the above given prediction. For samples 34 and 40,  $G_{xx}$  is a non-monotonic function of temperature with a maximum value of  $G_{xx}$  slightly lower than 1 around 3 K, corresponding to the case (iii). For sample 50,  $G_{xx} \approx 1$  does not change in the high-temperature range above 3 K and decreases at lower temperatures, corresponding to the case (ii). Note, the temperature dependences of  $G_{xx}$  are different for layers, which differ from each other only by thickness.

At magnetic fields near the spin-split QHE structure, the localization lengths  $\xi^\pm$  of the two spin systems are large because both spin systems are close to the quantum Hall state-insulator transition ( $|1/2 - G_{xy}^{\pm}| \ll 1$ ), where  $\xi^\pm \rightarrow \infty$ . Therefore, for the observation of the QHE with  $G_{xy} = 1$  a much lower temperature (or a larger coherence length) is necessary than for the QHE with  $G_{xy} = 2$ . In previous experiments at smaller magnetic fields [3] the spin-splitting was not observed, probably,

because at smaller fields  $\mu_B g B \partial G_{ij}^0 / \partial E$  is smaller. In our samples the spin-splitting is observed only at low temperatures  $T \lesssim 0.1$  K, what is much smaller than  $\hbar/\tau \approx 100$  K, and even than  $E_s/k_B \approx 4$  K.

The assumption about independent renormalization of the conductances of the two spin subbands is undoubtedly valid for non-interacting electrons in the absence of spin-flip scattering. Although electron-electron interaction is important in real systems, the experimental study of the flow diagram on samples 34, 40, and other thinner layers [14] shows good quantitative agreement with the predicted flow lines [7] for half the measured conductance values in the field range below 6 T, where there is not any manifestation of spin-splitting and, therefore,  $G_{ij}/2 = G_{ij}^+ = G_{ij}^-$ . This gives support for our model of independent spin-band contributions leading to the same critical points as for a spin-polarized system.

In summary, we observed spin-splitting in the QHE of heavily doped n-type GaAs layers with disorder much larger than spin-splitting  $g\mu_B B$ . Our results are in accordance with the scaling treatment of the quantum Hall effect, applied independently to the two spin subbands. Namely, the magnetic field position for the QHE is imposed by the occurrence of the Hall quantum value  $G_{xy} \approx 1$ , although this field position is only 1.5 times larger than the QHE field with  $G_{xy} = 2$ . Several features in the  $(G_{xy}, G_{xx})$  flow diagrams, like the observed critical values  $G_{xx}^c = 0.5 \pm 0.02$ ,  $G_{xy}^c = 0.5 \pm 0.05$  and  $1.5 \pm 0.05$  and the anomalous shapes of the flow lines, can be deduced from an independent summation of the contributions of the two spin bands. The spin-splitting is observed at temperatures  $T \lesssim 0.1$  K much smaller than all other energy scales determining the electron spectrum.

This work is supported by the Russian Foundation for Basic Research. We would like to thank B. Lemke for her help in the preparation of the samples.

- 
- [1] D. E. Khmel'nitskiĭ, *Helvetica Phys. Acta* **65**, 164 (1992).  
 [2] V. Kagalovsky, B. Horovitz, and Y. Avishai, *Phys. Rev. B* **55**, 7761 (1994), and references therein.  
 [3] H. W. Jiang, C. E. Johnson, K. L. Wang, and S. T. Hannahs, *Phys. Rev. Lett.* **71**, 1439 (1993); T. Wang, K. P. Clark, G. F. Spencer, A. M. Mack, and W. P. Kirk, *ibid.* **72**, 709 (1994); J. F. Hughes, J. T. Nicholls, J. E. F. Frost, E. H. Linfield, M. Pepper, C. J. B. Ford, D. A. Ritchie, G. A. C. Jones, E. Kogan, and M. Kaveh, *J. Phys. Condens. Matter* **6**, 4763; (1994); C. H. Lee, Y. H. Chang, Y. W. Suen, and H. H. Lin, *Phys. Rev. B* **58**, 10 629 (1998); C. F. Huang, Y. H. Chang, C. H. Lee, H. T. Chou, H. D. Yeh, C.-T. Liang, Y. F. Chen, H. H. Lin, H. H. Cheng, and G. J. Hwang, *Phys. Rev. B* **65**, 045303 (2001).  
 [4] R. J. Nicholas et al., *Phys. Rev. B* **37**, 1294 (1988), and references therein.  
 [5] A. P. Smith, A. H. MacDonald, and G. Gumbs, *Phys. Rev. B* **45**, 8829 (1992), and references therein.  
 [6] G. Murthy, *Phys. Rev. B* **64**, 241309 (2001).  
 [7] B. P. Dolan, *Nucl. Phys. B* **554**, 487 (1999); cond-mat/9809294.  
 [8] S. S. Murzin, M. Weiss, A. G. M. Jansen, and K. Eberl, *Phys. Rev. B* **64**, 233309 (2001).  
 [9] A. M. M. P. Pruisken, in *The Quantum Hall Effect*, edited by R. E. Prange and S. M. Girven, Springer-Verlag, 1990.  
 [10] D. E. Khmel'nitskiĭ, *Pis'ma Zh. Eksp. Teor. Fiz.* **38**, 454 (1983), [*JETP Lett.* **38**, 552 (1984)]; *Phys. Lett. A* **106**, 182 (1984).  
 [11] B. P. Dolan, *Phys. Rev. B* **62**, 10278 (2000).  
 [12] Y. Huo, R. E. Hetzel, and R. N. Bhatt, *Phys. Rev. Lett.* **70**, 481 (1993).  
 [13] Igor Ruzin and Shechao Feng, *Rev. Lett.* **74**, 154 (1995).  
 [14] S. S. Murzin, M. Weiss, A. G. M. Jansen and K. Eberl, *Phys. Rev. B* **66**, 233314 (2002).